Microwave cavity perturbation studies on H-form and ion-exchanged SCR catalyst materials: correlation of ammonia storage and dielectric properties

D. Rauch[1]*, M. Dietrich[1], T. Simons[2], U. Simon[2], A. Porch[3] and R. Moos[1]

[1]Department of Functional Materials, Bayreuth Engine Research Center (BERC), Zentrum für Energietechnik (ZET), University of Bayreuth, 95440 Bayreuth, Germany

[2] Institute of Inorganic Chemistry (IAC), RWTH Aachen University, 52074 Aachen, Germany

[3] School of Engineering, Cardiff University, Cardiff CF24 3AA, Wales, UK

* Functional.Materials@uni-bayreuth.de

Abstract

Ammonia-based selective catalytic reduction (SCR) has become the major control strategy for NO_x emissions from light and heavy duty diesel engines. Before reducing NO_x on the SCR active material, ammonia storage on the active sites of the catalyst is crucial. The *in operando* measurement of the dielectric properties of the catalyst material using microwave cavity perturbation is a promising indicator of ammonia loading. In this work, results on two zeolite-based SCR materials, i.e.ZSM-5 in H-form and copper ion-exchanged, are presented. The catalyst powder samples were monitored by microwave cavity perturbation as a function of ammonia content at a frequency of approximately 1.2 GHz in a temperature range between 200 and 350 °C. Due to ion exchange, the NH_3 storage behavior changes, what could be monitored in the sensitivity of the dielectric permittivity to NH_3. In addition, the dependence of the complex dielectric permittivity on ammonia loading is decreased by ion exchange, hinting that mostly ammonia storage on Brønsted sites affects the dielectric permittivity. This finding adds new knowledge to the electrical conduction and polarization mechanisms occurring in these zeolite materials.

Keywords

NH_3 storage, microwaves, cavity perturbation, zeolites, ZSM-5

Introduction

One of the continuously challenging factors for automotive manufacturers are the stringent emission standards of nitrogen oxides (NO_x) for combustion engines and the necessity to develop effective exhaust gas aftertreatment systems to meet the regulations. For leanly operated engines, mostly light and heavy duty diesel engines, in particular, ammonia-based selective catalytic reduction (SCR) has

become the major NO_x emission control strategy to meet actual and forthcoming emission standards [1]. Today, the focus for SCR-catalysts is on zeolites with active components like iron (Fe) and copper (Cu) [2,3]. In automotive applications, the ammonia-based SCR uses a non-toxic, aqueous urea solution (AdBlue™, DEF) as a reducing agent. The injected solution decomposes by hydrolysis to ammonia (NH_3) and carbon dioxide (CO_2) in the hot exhaust. Before the SCR reactions take place, a previous NH_3 adsorption on the acidic sites on the zeolite surface is an essential precondition. This NH_3 storage ability also offers the benefit to buffer changes of flow and temperature in order to ensure a permanent NO_x conversion. The catalyst reduces NO_x selectively to nitrogen (N_2) and water (H_2O). The two main SCR reactions are shown in the following: the "standard" SCR reaction (Eq. 1) with NO and the "fast" SCR reaction (Eq. 2) with equimolar amounts of NO and NO_2 [4]:

$$4NH_3 + 4NO + O_2 \rightarrow 4N_2 + 6H_2O \quad (1)$$

$$4NH_3 + 2NO + 2NO_2 \rightarrow 4N_2 + 6H_2O \quad (2)$$

Both, the capacity to store NH_3 and the catalytic activity of zeolite SCR catalysts show a strong dependence on the number and the strength of the acid sites of the zeolite (Lewis and Brønsted sites). Basically, NH_3 adsorption can occur strongly on Brønsted acid sites and weakly as a coordination layer around the strongly bound species via hydrogen bonds or on Lewis sites [5,6]. Due to chemical NH_3 adsorption, the proton conductivity of the zeolite increases distinctly. Due to the different mechanisms, it depends on temperature in a non-Arrhenius manner [5,7]. In order to determine the number of acid sites, temperature-programmed desorption (TPD) of NH_3 is common, but an unambiguous discrimination between Lewis and Brønsted sites is still not possible [8]. Therefore, the approach to correlate dielectric properties under reaction conditions with the catalytic and NH_3 storage behavior *in situ* holds promise for additional information to identify acidic sites or optimize the catalyst material. Here, the cavity perturbation method, which uses microwaves in the GHz range, is suitable, not least because it is non-invasive (apart from interaction with a low power microwave field) and contactless.

Recently, a similar approach closer to automotive on-road applications has been suggested, examining serial-type catalyst devices (as applied in exhaust gas aftertreatment systems with volumes of about 1.5 to 2 liters) [9]. Since the metal canning of the catalyst is used as cavity resonator, the sample occupied most of the cavity volume. Hence, these systems are suitable for real-world applications but not to characterize material properties owing to their very large perturbation of the sample on the cavity space. Already, successfully tested applications include the determination of the oxygen loading of three-way catalytic converters [9-12], or the soot loading [13,14] or ash loading [15] of full-sized diesel particulate filters. The storage degree of NO in lean NO_x traps [10,16] and the NH_3 loading on SCR catalyst devices have also been successfully monitored [17,18,19] using the cavity perturbation method.

In a previous work, a laboratory test setup for catalyst powder characterization under reaction conditions by microwave cavity perturbation with the ability to determine the dielectric properties of catalyst material *in operando* was developed [20]. It enables the direct measurement of the complex permittivity of catalytic powder samples undergoing gas storage and catalytic reactions in a defined gas atmosphere,

with gas analyzers up- and downstream of the catalyst sample. In the actual, improved version, it operates within a temperature range from room temperature (where usually no reactions occur) to 400 °C.

Methods

In this work, a microwave cavity perturbation technique operating at approximately 1.2 GHz was applied for material characterization, which uses standing electromagnetic waves (i.e. resonances) inside a defined, hollow cylindrical shaped aluminum cavity. The insertion of a small sample into the cavity resonator leads to a minor perturbation of the electromagnetic field distribution. To determine the dielectric permittivity of the sample, the latter is placed within a region of maximum electric field (and zero magnetic field). For the TM_{010} mode, which is analyzed in this work, this region is along the entire cylinder axis. The resulting decrease of the resonance frequency and the increase of the 3 dB bandwidth (i.e. decrease of the quality factor Q) of the resonance curve are related to real and imaginary parts, respectively, of the complex dielectric permittivity $\varepsilon = \varepsilon_1 - j\varepsilon_2$ of the sample: the real part ε_1 (or, more properly, ε_1 - 1) quantifies the polarization of the material and the imaginary part ε_2 quantifies the dielectric loss. Together with the volume of the sample V_s and the mode volume of the resonator V_{eff} (which for the TM_{010} mode is 26.9% of the enclosed volume of the cylinder), the complex dielectric permittivity can be calculated using equations 3 and 4 [21].

$$\frac{(f_0 - f_s)}{f_0} \approx (\varepsilon_1 - 1)\frac{V_s}{2V_{eff}} \tag{3}$$

$$\frac{1}{Q_s} - \frac{1}{Q_0} = \Delta\left(\frac{1}{Q}\right) \approx \varepsilon_2 \frac{V_s}{V_{eff}} \tag{4}$$

The resonance peak in the frequency spectrum of the transmission parameter S_{21}, together with the parameters considered for microwave analysis, are shown in Fig. 1(a), namely: the resonance frequency with sample f_s, the 3 dB (or “half-power”) bandwidth BW, and the peak height $|S_{21,max}|$. To calculate ε_1 from Eq. 3, the resonance frequency shift is used and for the calculation of ε_2 by Eq. 4, the unloaded quality factor Q is required, from which the effects of cavity coupling have been removed. The used (and in [20] described) cavity is designed (and measured) to have symmetric coupling, i.e. equal inductive coupling strength at each of its two ports, so the coupling unloading process can be calculated using Eq. 5 [21].

$$Q = \frac{f}{BW}\left(1 - 10^{-|S_{21,max}|/20}\right) \tag{5}$$

where the value of resonant frequency is f_0 for calculation of Q_0 (without the sample), or f_s for calculation of Q_s (with the sample). In this work, the microwave parameters were determined by a complex analysis approach using the frequency-phase relation for significantly higher measurement accuracy compared to scalar Lorentzian type curve fitting [22,23].

The microwave parameters were measured using a vector network analyzer (Anritsu Shockline MS46322A). The effects on the transmission signal are displayed in Fig. 1(b). The peak of the empty cavity (black) shifts to a lower frequency and decreases slightly in peak height as the sample is inserted (red). The NH_3 saturated sample leads to an additional frequency shift and to a stronger decrease in peak height.

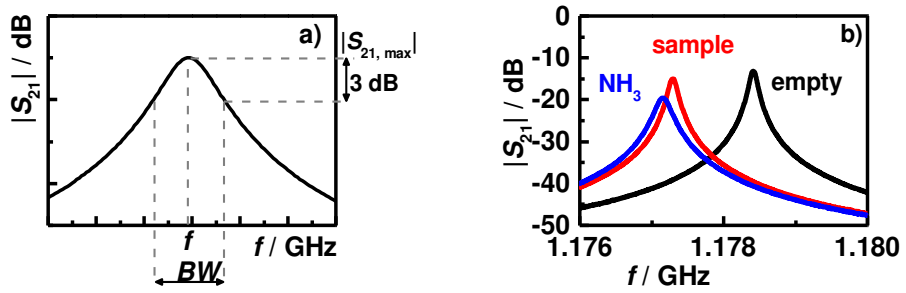

Figure 1 (a) An exemplary resonance peak in detail, showing the resonant frequency *f*, 3 dB bandwidth *BW*, and maximum peak height $|S_{21,\,max}|$, (b) resonance peaks at 200 °C of the empty sample tube (black), with inserted H-ZSM-5 sample (red), and with the H-ZSM-5 sample loaded with NH_3 (blue)

The zeolite under test was a H-ZSM-5 powder with a Si/Al ratio of 27 (Clariant International Ltd.). The Cu-ZSM-5 was prepared by aqueous ion-exchange of the H-ZSM-5. The Cu ion-exchange level was determined to an atomic ratio of Cu:Al of 0.11 by EDX. Both samples were weighted and their skeletal volumes were determined using a helium gas pycnometer. All measurements were performed on a test bench setup described in [20] with a total gas flow of 1 l/min and a background gas composition of 2 % H_2O balanced with N_2. All gas flows were controlled by mass flow controllers (MFCs, MKS) and the downstream gas concentrations were monitored by a Fourier Transformed Infrared Spectroscopy (FTIR) analyzer (Nicolet Antaris IGS).

Results and Discussion

Figure 2 shows a storage measurement on H-ZSM-5 at 200 °C. In Fig. 2(a), the inlet (MFC data, dashed) and outlet (FTIR data, solid) gas concentrations of NH_3, NO, NO_2 and N_2O are shown. From these data, the adsorbed amount of NH_3 on the zeolite is calculated and is shown in mg per gram of sample in Fig. 2(c). In Fig. 2(b), the measured real and imaginary parts of the permittivity are presented. After 10 minutes in background gas (at t_1), 500 ppm NH_3 were fed and immediately, both parts of the permittivity are seen to increase due to the adsorption of NH_3. Initially, the zeolite stores all of the incoming NH_3, indicated by the fact that no NH_3 can be detected downstream by the FTIR analyzer. After 65 minutes (at t_2), the NH_3 concentration downstream almost reached the inlet concentration and the permittivity values remained at a constant level, indicating that the catalyst was saturated with NH_3. Thus, NH_3 was turned off and the weakly bound NH_3 was desorbed or released during the following 90 minutes, seen in a slow decrease in the downstream concentration of NH_3 and the permittivity. When no NH_3 was detected downstream anymore (at t_3), 10 % O_2, 250 ppm NO and 250 ppm NO_2 were admixed to convert

the remaining strongly bonded NH_3 according to the "fast" SCR reaction (Eq. 2), until the zeolite was free of NH_3 (at t_4) as the overall NO_x concentration downstream reached the inlet concentration and the permittivity returned to its values of the beginning of the measurement. One clearly can see the good correlation between the stored amount and the measured complex permittivity.

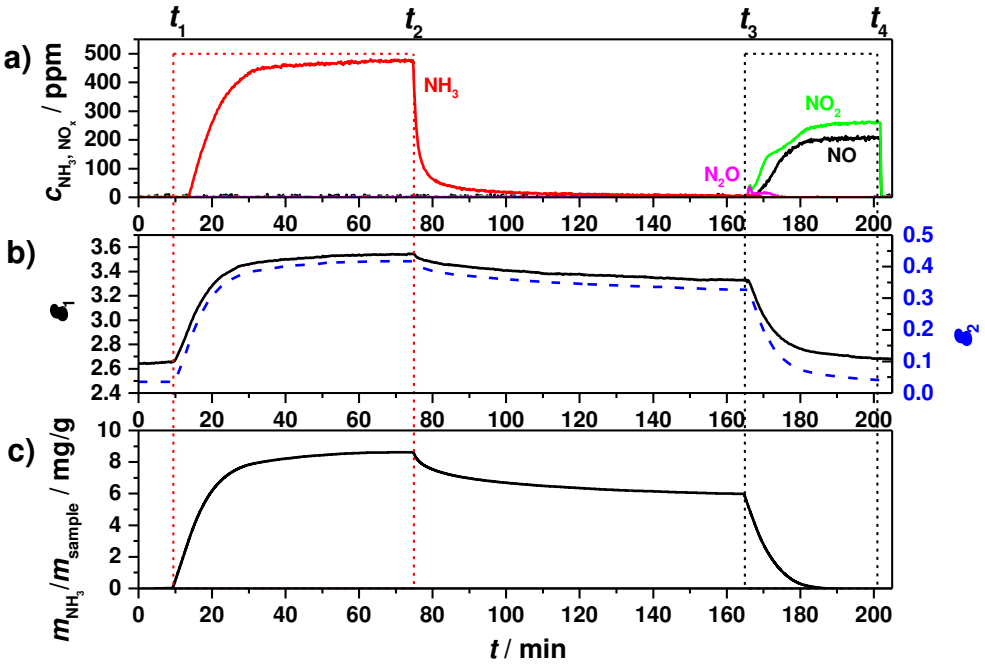

Figure 2 Storage measurement on H-ZSM-5 at 200 °C. (a) Inlet (dashed) and outlet (solid) gas concentrations of NH_3 (red), NO (black) and NO_2 (green) and N_2O (magenta), (b) real (black) and imaginary (blue, dashed) part of the permittivity and (c) calculated amount of NH_3 adsorbed on the catalyst

The same experiment as shown in Fig. 2 was performed at temperatures of 200, 250 300 and 350 °C on the H-form and the Cu exchanged ZSM-5 sample with inlet concentrations of NH_3 of 250 and 500 ppm. For the subsequent analysis, three steady states were evaluated for each measurement: the NH_3 free condition at the beginning of the measurement, the saturated state (at t_2), where the total stored amount was determined, and the point when the free desorption was finished (at t_3), where the strongly bound fraction was identified. In Fig. 3, ε_1 and ε_2 are plotted at the three mentioned states over the adsorbed amount on the H-ZSM-5 powder. Measurements with an NH_3 inlet concentration of 250 ppm (open symbols) and 500 ppm (filled) are shown at different temperatures. One can see, especially in the plot of ε_2, that the total stored amount of NH_3 reduces with increasing temperature from 8.6 mg per g powder sample at 200 °C to 2.4 mg/g at 350 °C for an inlet concentration of 500 ppm. Furthermore, it is apparent that the total adsorbed amount is dependent on the partial pressure of NH_3, as the total stored amount for the inlet concentration of 250 ppm is lower than for 500 ppm, especially at the higher temperatures, were NH_3 is mainly weakly bound. The strongly bound fraction of NH_3 is only dependent on the number of Brønsted acid sites, which can be seen by the almost identical values of strongly bound NH_3 for 250 and 500 ppm. ε_1 without ammonia has values between 2.2 and 2.7, but is decreasing with temperature. For all temperatures, ε_1 increases linearly with the stored mass of NH_3, with a slope

slightly increasing with temperature. ε_2 is almost zero in the unloaded state at each temperature, as the zeolite is an almost lossless material. The dielectric losses increase linearly with stored NH_3 and show a higher dependency on temperature compared to ε_1, as the slopes increase more strongly with increasing temperature.

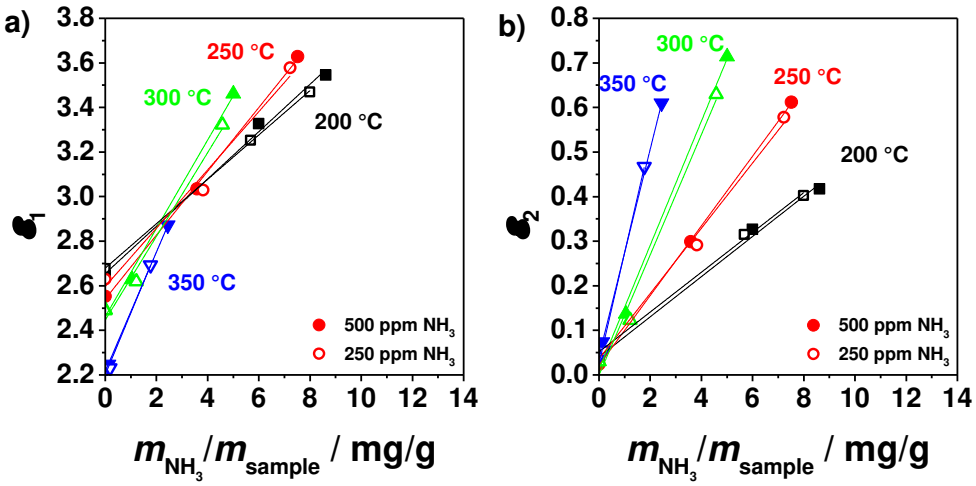

Figure 3 (a) ε_1 and (b) ε_2 as a function of stored amount of NH_3 for H-ZSM-5 at 200 °C (black), 250 °C (red), 300 °C (green) and 350 °C (blue) for measurements with 250 ppm (open symbols) and 500 ppm (filled) inlet concentration of NH_3

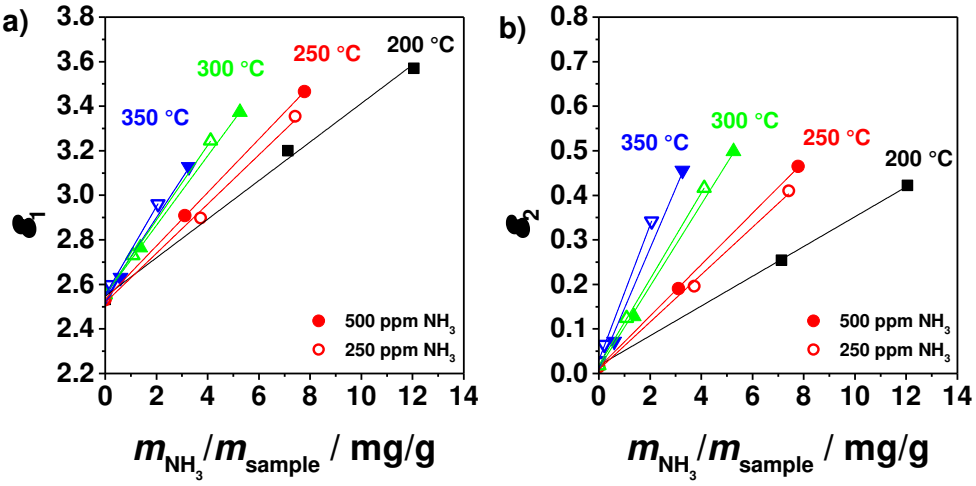

Figure 4 (a) ε_1 and (b) ε_2 over stored amount of NH_3 for Cu-ZSM-5 at 200 °C (black), 250 °C (red), 300 °C (green) and 350 °C (blue) for measurements with 250 ppm (open symbols) and 500 ppm (filled) inlet concentration of NH_3

In Fig. 4, the same measurements are shown on the Cu exchanged samples, except for the missing data at 200 °C with 250 ppm inlet concentration. The total stored amount of NH_3 at 200 °C is higher for this sample compared to the H-form, what is caused by the weak storage on the Cu ions, which can be coordinated by up to four NH_3 molecules [24]. At higher temperatures, the NH_3 storage is on the same level as the storage on the H-form. Again, one can see the dependencies on temperature and NH_3 partial pressure of the total stored amount. The unloaded ε_1 takes similar values to the H-form sample

between 2.5 and 2.6, showing no strong temperature dependence in the unloaded state compared to the H-form. The basic behavior of the slopes for ε_1 appear comparable for both samples. ε_2 shows again a higher temperature dependency than ε_1, but the overall dielectric losses are smaller than for the H-form. A possible reason therefore is that the losses are predominantly caused by this adsorbed NH_3, which is strongly bound to the Brønsted acid sites.

For a better comparison of the two materials, the changes of ε_1 and ε_2 between unloaded and saturated state referred to the total stored amount of NH_3, hereafter called sensitivity $S = \Delta\varepsilon/(m_{NH3}/m_{sample})$, were calculated and are shown in Fig. 5. S_1 (a) and S_2 (b) increase with temperature, which is caused by the thermal activation of the NH_4^+ ions, as they become more mobile at higher temperatures. The sensitivities of both permittivity values are higher for the H-form, compared to the Cu-ZSM-5. An explanation therefore could be that the NH_3 species which are coordinatively bound to the copper sites do not influence the permittivity to a large extent. The values for loading with 250 and 500 ppm NH_3 are nearly similar at each temperature, so that the change of the permittivity is only dependent on the stored amount of NH_3.

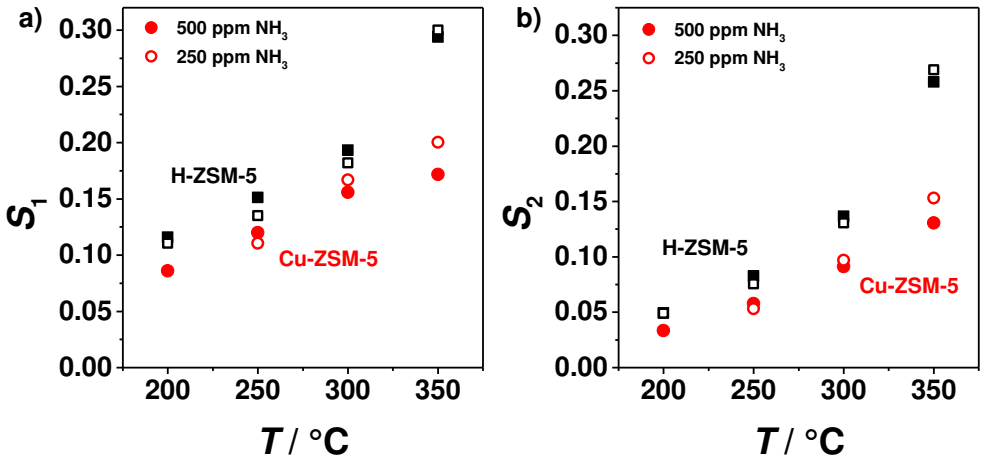

Figure 5 Sensitivities of (a) ε_1 and (b) ε_2 for H-ZSM-5 (black) and Cu-ZSM-5 (red) for NH_3 inlet concentrations of 250 ppm (open symbols) and 500 ppm (filled)

Conclusion and Outlook

In this study, initial measurements with a recently introduced measurement setup using microwave cavity perturbation for catalyst powder samples were performed on ZSM-5 zeolites in H-form and Cu exchanged. The selected temperature range was 200 °C to 350 °C and all measurements were performed with 2 % water. For both samples, the amount of stored NH_3 was mirrored by both the real ε_1 and the imaginary parts ε_2 of the complex dielectric permittivity. In storage, both samples behave similarly, the only exception being the Cu exchanged zeolite at 200 °C, which shows significantly higher storage. This might be related to the coordinative binding of NH_3 to Cu ions at lower temperatures. The H-form shows continuously higher sensitivities of the complex dielectric permittivity to NH_3 compared to the Cu exchanged sample. A possible explanation is that storage on Cu ions might have only a weak

effect on the measurable dielectric properties compared to storage on Brønsted sites. However, this experimental finding requires further investigations.

In future work, samples with other exchanged ions like iron (Fe) and varying exchange levels will be investigated. Another focus is to perform temperature-programmed desorption experiments. Additionally, frequency dependent measurements of the complex permittivity by analyzing several cavity modes (from 1.1 GHz to 4.2 GHz) are planned.

Acknowledgments

R.M. is indebted to the German Research Foundation (DFG) for supporting this work under grant MO 1060/19-1.

U.S. acknowledges financial supported by the German Research Foundation (DFG), contract No: Si609/14-1, and by the Exploratory Research Space of RWTH Aachen University within the Center for Automotive Catalytic Systems Aachen (ACA).

A.P. acknowledges the support of Merck GKaA.

References

[1] Johnson TV (2009) Review of diesel emission and control (2009) Int. J. Engine Res. Doi: 10.1243/14680874jer04009

[2] Rahkamma-Tolonen K, Maunula T, Lomma M, Huuhtanen M, Keiski RL (2005) The effect of NO2 on the activity of fresh and aged zeolite catalysts in the NH3-SCR reaction. Catal. Today. Doi: 10.1016/j.cattod.2004.09.056

[3] Di Iorio JR, Ribeiro FH, Bates SA, Verma AA, Miller JT, Gounder R (2015) The Dynamic Nature of Brønsted Acid Sites in Cu–Zeolites During NOx Selective Catalytic Reduction: Quantification by Gas-Phase Ammonia Titration. Top. Catal. Doi: 10.1007/s11244-015-0387-8

[4] Koebel M, Elsener M, Kleemann M (2000) Urea-SCR: a promising technique to reduce NOx emissions from automotive diesel engines. Catal. Today. Doi: 10.1016/s0920-5861(00)00299-6

[5] Rodriguez-Gonzalez L, Rodriguez-Castellon E, Jimenez-Lopez A, Simon U (2008) Correlation of TPD and impedance measurements on the desorption of NH3 from zeolite H-ZSM-5. Solid State Ionics. Doi:10.1016/j.ssi.2008.06.007

[6] Giodanino F, Borfecchia E, Lomachenko K, Lazzarini A, Agostini G, Gallo E, Soldatov AV, Beato P, Bordiga S, Lamberti C (2014) Interaction of NH3 with Cu-SSZ-13 Catalyst: A Complementary FTIR, XANES, and XES Study. J. Phys. Chem. Lett. Doi:10.1021/jz500241m

[7] Franke M, Simon U (2004) Solvate-Supported Proton Transport in Zeolites. ChemPhysChem. Doi:10.1002/cphc.200301011

[8] Niwa M, Katada N (2013) New Method for the Temperature-Programmed Desorption (TPD) of Ammonia Experiment for Characterization of Zeolite Acidity: A Review. Chem. Record. Doi: 10.1002/tcr.201300009

[9] Moos R, Beulertz G, Reiß S, Hagen G, Votsmeier M, Fischerauer G, Gieshoff J (2013) Overview of the Microwave-Based Automotive Catalyst State Diagnosis. Top. Catal. Doi: 10.1007/s11244-013-9980-x

[10] Moos R, Wedemann M, Spörl M, Reiß S, Fischerauer G (2009) Direct Catalyst Monitoring by Electrical Means: An Overview on Promising Novel Principles. Top. Catal. Doi: 10.1007/s11244-009-9399-6

[11] Beulertz G, Herbst F, Hagen G, Fritsch M, Gieshoff J, Moos R (2013) Microwave Cavity Perturbation as a Tool for Laboratory In Situ Measurements of the Oxidation State of Three Way Catalysts. Top. Catal. Doi: 10.1007/s11244-013-9987-3

[12] Reiß S, Wedemann M, Spörl M, Fischerauer G, Moos R (2011) Effects of H2O, CO2, CO, and flow rates on the RF-based monitoring of three-way catalysts. Sens. Lett. Doi: 10.1166/sl.2011.1472

[13] Sappok A, Parks J, Prikhodko V (2010) Loading and Regeneration Analysis of a Diesel Particulate Filter with a Radio Frequency-Based Sensor. SAE Technical Paper. Doi: 10.4271/2010-01-2126

[14] Feulner M, Hagen G, Moos R, Piontkowski A, Müller A, Fischerauer G, Brüggemann D (2013) In-Operation Monitoring of the Soot Load of Diesel Particulate Filters: Initial Tests. Top. Catal. Doi: 10.1007/s11244-013-0002-9

[15] Kulkarni VP, Leustek ME, Michels SK, Nair RN, Snopko MA, Knitt AA (2013) Ash Detection in Diesel Particulate Filter. U.S. Patent 8,470,070 B2

[16] Fremerey P, Reiß S, Geupel A, Fischerauer G, Moos R(2011) Determination of the NOx Loading of an Automotive Lean NOx Trap by Directly Monitoring the Electrical Properties of the Catalyst Material Itself. Sensors. Doi: 10.3390/s110908261

[17] Reiß S, Schönauer D, Hagen G, Fischerauer G, Moos R (2011) Monitoring the Ammonia Loading of Zeolite-Based Ammonia SCR Catalysts by a Microwave Method. Chem. Eng. Technol. Doi: 10.1002/ceat.201000546

[18] Rauch D, Kubinski D, Simon U, Moos R (2014) Detection of the ammonia loading of a Cu Chabazite SCR catalyst by a radio frequency-based method. Sens. Actuators B. Doi:10.1016/j.snb.2014.08.019

[19] Rauch D, Kubinski D, Cavataio G, Upadhyay D (2015) Ammonia Loading Detection of Zeolite SCR Catalysts using a Radio Frequency based Method. SAE Int. J. Engines. Doi: 10.4271/2015-01-0986

[20] Dietrich M, Rauch D, Porch A, Moos R (2014) A laboratory test setup for in situ measurements of the dielectric properties of catalyst powder samples under reaction conditions by microwave cavity perturbation: set up and initial tests. Sensors. Doi: 10.3390/s140916856

[21] Porch A, Slocombe D, Beutler J, Edwards P, Aldawsari A, Xiao T, Kuznetsov V, Almegren H, Aldrees S, Almaqati N (2012) Microwave treatment in oil refining. Appl. Petrochem. Res. Doi: 10.1007/s13203-012-0016-4

[22] Inoue R, Miwa K, Kitano H, Maeda A, Odate Y, Tanabe E (2004) Highly Accurate and Real-Time Determination of Resonant Characteristics: Complex Linear Regression of the Transmission Coefficient. IEEE Trans. Microwave Theory Techn. Doi: 10.1109/TMTT.2004.834183

[23] Leong K, Mazierska J (2002) Precise measurements of the Q factor of dielectric resonators in the transmission mode-accounting for noise, crosstalk, delay of uncalibrated lines, coupling loss, and coupling reactance. IEEE Trans. Microwave Theory Techn. Doi: 10.1109/TMTT.2002.802324

[24] Komatsu T, Nunokawa M, Moon IS, Takahara T, Namba S, Yashima T (1994) Kinetic Studies of Reduction of Nitric Oxide with Ammonia on Cu2+-Exchanged Zeolites. J. Catal. Doi:10.1006/jcat.1994.1229